The effect of different lower detection thresholds in microdosimetric spectra and their mean values

DOI: 10.1016/j.radmeas.2021.106626
Handle: http://hdl.handle.net/1942/34506

The effect of different lower detection thresholds in microdosimetric spectra and their mean values

A. Bianchi[a,b,c], A. Selva[c], P. Colautti[c], A. Parisi[a], F. Vanhavere[a], B. Reniers [b], V. Conte[c]

[a] *Belgian Nuclear Research Centre SCK CEN, Boeretang 200, 2400 Mol, Belgium*

[b] *University of Hasselt, Faculty of Engineering Technology, Centre for Environmental Sciences, Nuclear Technology Center, Agoralaan, 3590 Diepenbeek, Belgium*

[c] *Istituto Nazionale di Fisica Nucleare INFN, Laboratori Nazionali di Legnaro, viale dell'Università 2, Legnaro (Padova), Italy*

Corresponding author: Bianchi Anna – anna.bianchi@sckcen.be

Keywords: Microdosimetry, mini-TEPC, Particle Therapy, Linear extrapolation

Abstract

Research on the applications of microdosimetry to particle therapy is spreading worldwide with a rapid increase of publications in the last years. In order to be able to perform an intercomparison of data acquired with different detectors in different clinical centres it is important to analyse data with a standard procedure. Often microdosimetric spectra are presented with different lower detection thresholds, in relation with different detection sensitivity and noise levels. The purpose of this paper is to analyse the influence of the lower detection threshold on the dose-mean lineal energy values, which are used as an assessment of the average LET of the radiation field. Furthermore, the dose distribution of the lineal energy can be used in combination with biological weighting functions to estimate the biological RBE at different positions along the penetration depths of therapeutic proton or carbon ion beams. Microdosimetric spectra cut at different lower thresholds lead in principle to different RBE values. It was an additional purpose of this work to analyse and discuss this effect both for proton and carbon ion irradiations.

Spectra in proton and carbon ion beams gathered with a miniaturized TEPC developed at the Legnaro National Laboratories of the Italian Institute for Nuclear Physics (LNL-INFN) have been used to perform this study.

Linear extrapolation of the microdosimetric spectra to a common value of 0.01 keV/μm significantly reduces the deviations in the mean values due to different lower thresholds. It is advisable to perform this procedure to uniform the data analysis and facilitate the intercomparison of data.

1. Introduction

Microdosimeters measure the stochastic process of energy deposition in a micrometric target aiming to mimic the radiation interaction process in a cell. The stochastic nature of the interaction is likely related to the biological effectiveness of different radiation fields, with densely ionizing radiation more effective than sparsely ionizing radiation, for a given absorbed dose [Rossi, 1966; Durante, 2009].

The interest in microdosimetry for potential application in hadron therapy, as a tool to measure the radiation quality of complex radiation fields, is growing worldwide, as documented by the increasing number of publications on this topic. Several detectors, both typical Tissue Equivalent Proportional Counters (TEPCs) and solid-state microdosimeters are currently being used to study the radiation quality of different clinical centres [Conte et al., 2020]. In order to make the intercomparison of results, between each other and with meaningful simulated data, it is important to set a standard procedure for data analysis. In particular, the dose-mean lineal energy, $\bar{y}_D$, is defined in the ICRU Report 36 [Booz J., 1983] as the mean values of the dose distributions $d(y)$ of the lineal energy over the whole range of lineal energy values. However, electronic noise and detection system sensitivity pose a limit on the lowest detectable signal, the signal that can be detected over the background electronic noise of the detection system. The main source of noise is the preamplifier, with typical noise levels of 500 electrons RMS. The minimum detectable signal ε_m (or Lower Level Discriminator (LLD)) should be set to about 5 times the RMS noise to avoid the conversion of background noise pulses and freezing of the acquisition system [H. Rossi and M. Zaider, 1996; D. Srdoc, 1970]:

$$\varepsilon_{min} = \frac{5 \cdot e_{\mathrm{rms}} \cdot W}{G} \tag{1}$$

where W is the average energy required to produce an ion pair (electron-hole pair in case of solid state detectors), approximately 10/3.6/28 eV for diamond/silicon/propane gas respectively, and G is the amplification factor of the detector, which is 1 for solid state detectors and about 500 for gas proportional counter. When this rule is followed most of the noise is suppressed with 1 count per second as counting rate for the background noise. According to equation (1) and with e_{rms}=500, the minimum detectable energy in diamond and silicon microdosimeters results to be $\varepsilon_{\mathrm{min}} = 25\ \mathrm{keV}$ and $\varepsilon_{\mathrm{min}} = 9\ \mathrm{keV}$ respectively. In terms of lineal energy, these $\varepsilon_{\mathrm{min}}$ values correspond to $y_{\mathrm{min}} = \varepsilon_{\mathrm{min}}/\bar{l}$, being $\bar{l}$ the mean chord length of the sensitive volume. Therefore, for a given RMS noise, the actual value y_{min} decreases with increasing simulated site size. For instance, if $\bar{l} = 10\ \mu\mathrm{m}$ one gets $y_{\mathrm{min}} = 2.5\ \mathrm{keV}/\mu\mathrm{m}$ and $y_{\mathrm{min}} = 0.9\ \mathrm{keV}/\mu\mathrm{m}$ ion correspondence of the previous values of $\varepsilon_{\mathrm{min}}$.

For a spherical TEPC simulating a water site of 1 μm, having a typical gas gain G=500, the minimum detectable energy is $\varepsilon_{\mathrm{m}} = 0.14$ keV and the minimum lineal energy is $y_{\mathrm{min}} = 0.21$ keV/μm.

To minimize the dependency on the lower detection threshold of the average lineal energy values, the lineal energy distributions can be linearly extrapolated down to a common threshold of 0.01 keV/μm, corresponding to the ionization threshold of 10 eV in water. This extrapolation procedure is described in [Lindborg and Waker, 2017], [Lindborg, 1975] [Beck et al., 2004] and it has been normally applied in other publications of the mini-TEPCs [Conte et al., 2020] [Bianchi et al., 2020] together with a discussion on the uncertainties related to this procedure [Moro et al., 2003a] [Moro et al., 2003b]. However, this extrapolation procedure is not applied often by experimental groups (see for example Missiaggia et al., 2020; Verona et al, 2020; Debrot et al., 2018), leading to a heterogeneity of results that strongly depend on the electronic noise level during the irradiation and on the specific detector sensitivity. When the lineal energy mean values are calculated from microdosimetric distributions that are cut above the lowest detectable signal without performing the extrapolation to 0.01 keV/μm, the low lineal energy fraction of the microdosimetric spectrum is completely neglected resulting in artificially higher values of the calculated mean values. The *yd(y)* distributions measured with thick silicon detectors or with diamond microdosimeters, often show a cut at about 1 keV/μm (see for example Debrot et al., 2018; Verona et al., 2020). The lowest detectable signal, in terms of lineal energy, for thin silicon devices can be up to 10 times higher [Agosteo et al., 2010].

In this work, we studied the influence of the lower detection threshold on the calculated dose-mean lineal energy values and also on the assessment of the Relative Biological Effectiveness (RBE) for clonogenic survival of asynchronized normoxic V79 cells, calculated with a new Biological Weighting Function by [Parisi et al., 2020]. The analysis was performed on microdosimetric spectra measured with protons and carbon ion beams with a miniaturized TEPC.

2. Material and Methods

2.1 The detector: mini-TEPC

The mini-TEPC which was employed in the measurement campaign at the Centre for Hadron Therapy and Advanced Nuclear Applications (CATANA, Catania, Italy) beam line has been developed at the LNL-INFN and is an upgrade of the version described in [De Nardo et al., 2004] that measured at National Centre for Oncological Hadron therapy (CNAO, Pavia, Italy). This mini-TEPC was modified in order to

work without gas flow [Conte et al., 2019] and for this reason all the gas ducts have been enlarged and more attention has been paid to vacuum tightness during the machining and assembly operations.

The cylindrical sensitive volume is 0.9 mm in diameter and height, the decision of developing such a small detector was mainly due to the intention of measuring in clinical beams, where the particle fluence is high and often cannot be reduced.

The cathode surrounding the sensitive volume is made of a cylinder of A150 plastic 0.35 mm thick, the anode, which is a 10 µm thick gold-plated tungsten wire, is located on the central axis of the sensitive volume.

Externally, a 0.35 mm thick Rexolite® shell is used to insulate the cathode from the 0.2 mm thick titanium sleeve that encloses the detector. The overall external diameter is 2.7 mm (see Figure 1). The total water equivalent thickness was calculated as 1.37 mm [Conte et al., 2019] considering the ratio of the stopping powers of protons in the different materials and water.

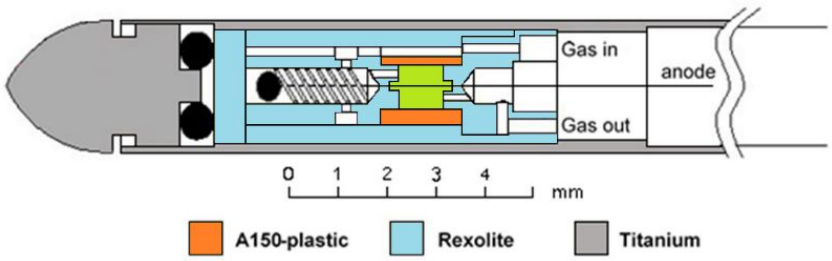

Figure 1 – Section of the upgraded detector.

The detector is filled with pure propane at an internal gas pressure of 45.4 kPa that corresponds to a site size of 0.75 µm in propane when scaled at density 1 g /cm³, this pressure was chosen for consistency with previous measurements and corresponds to 1 µm in tissue. The pressure was controlled with an absolute pressure transducer MKS Baratron type 722A.

The mini-TEPC detector is coupled with a custom-made low noise charge-sensitive preamplifier that has a dynamic range higher than 4 orders of magnitude. The output of the preamplifier is sent to two different linear pulse-shaping amplifiers with different gains in order to increase the resolution on smaller signals. The Gaussian shaped signals are digitalized by two different ADCs and sent to the acquisition PC.

The sub-spectra obtained from the two electronic chains are then joined offline in the overlapping region into one unique spectrum. All spectra are calibrated in lineal energy referring to water.

2.2 Measurement and data analysis

Following definitions of ICRU report 36 [ICRU Report 36, 1983], the dose-weighted distribution of the lineal energy obey the usual normalization condition of probability distributions:

$$\int_0^\infty d(y)\mathrm{d}y = 1 \qquad (2)$$

The mean value of the dose distributions are calculated through the following equation (3):

$$\bar{y}_D = \int_0^\infty y d(y)\mathrm{d}y \qquad (3)$$

When dealing with experimental data, the lower integration limit in equations (1) and (2) is replaced y_{min}, which represents either the actual minimum detectable signal or alternatively the extrapolation limit $y_{min} = 0.01\,\mathrm{keV/\mu m}$. The new equations are given below:

$$\int_{y_{min}}^\infty d(y)\mathrm{d}y = 1 \qquad (4) \qquad\qquad \bar{y}_D = \int_{y_{min}}^\infty y d(y)\mathrm{d}y \qquad (5)$$

Microdosimetric measurements were performed at the 62 MeV modulated proton beam of CATANA [Cirrone et al., 2004] at eleven positions across the proton penetration depth. The beam is a half-modulated Spread Out Bragg Peak that is 1.1 cm wide, and the maximum range in water is at a depth of 2.9 cm (the dose profile is shown in the left panel of Figure 3). The lineal energy calibration of experimental spectra was performed via the proton-edge technique, assigning to the flex position of the fitted Fermi function the value of 143 keV/μm [Bianchi et al., 2021]. Due to electromagnetic noise in the clinical environment, the minimum detectable signal above noise level was 0.35 keV/μm.

The experimental frequency data were extrapolated to 0.01 keV/μm by the linear best fit of experimental *f(y)* distributions in the lineal energy range between 0.35 and 0.45 keV/μm. The frequency and dose mean lineal energy values were calculated from extrapolated spectra using equation (4) with y_{min}=0.01 keV/μm, and compared with the correspondent mean values obtained from the original distributions, with the detection threshold at 0.35 keV/μm and without the extrapolation. In order to simulate other noise conditions, different thresholds have been introduced and applied to the spectra. The average values obtained with the new thresholds and after the linear extrapolation procedure have been calculated also for these conditions and compared. The maximum threshold value analysed was 1.0 keV/μm, a value that does not neglect peaks in the dose distributions of the lineal energy *d(y)*, and an intermediate value of 0.7 keV/μm was also considered. In correspondence of these two higher thresholds, two additional

extrapolations from linear best fit of frequency data in the lineal energy ranges 0.7-0.8 keV/µm and 1-1.2 keV/µm were performed.

Microdosimetric spectra measured in a 189.5 MeV/u carbon ion beam at CNAO and published in [Conte et al., 2012] have been also processed to calculate $\bar{y}_D$. In this case, due to electromagnetic noise in the clinical environment, the minimum detectable signal above noise level was 0.4 keV/µm.

For carbon ions the thresholds analysed are: 0.4, 0.7, 1.0, 4.0 and 10 keV/µm. The minimum value corresponds to the minimum detectable signal experimentally found during the measurement campaign, the highest to the maximum threshold that does not cut peaks in the dose distribution of the lineal energy *d(y)*, three intermediate values were chosen in between. The mean values $\bar{y}_D$ have been calculated both for the spectra with the component under the threshold cut off and neglected , and from spectral distributions extrapolated to y_{min}=0.01 keV/µm by linear best fit of the distributions in the intervals 0.4-0.5 keV/µm, 0.7-0.8 keV/µm, 1-1.2 keV/µm, 4-5 keV/µm and 10-12 keV/µm.

A summary of the lower detection thresholds and fitting *y*-intervals considered for extrapolating the distributions to *y* = 0.01 keV/µm is listed in Table 1.

Threshold	**Extrapolation interval**
0.35 keV/µm (protons only)	0.35-0.45 keV/µm
0.7 keV/µm	0.7-0.8 keV/µm
1 keV/µm	1-1.2 keV/µm
0.4 keV/µm (carbon ions only)	0.4-0.5 keV/µm
4 keV/µm (carbon ions only)	4-5 keV/µm
10 keV/µm (carbon ions only)	10-12 keV/µm

Table 1 – Lower thresholds and fitting intervals for the extrapolation procedure.

The relative variation between dose-mean lineal energy values derived from cut and extrapolated distributions, at different threshold levels, has been calculated with respect to the most precise mean value that is the one obtained by extrapolating to 0.01 keV/µm the experimental distribution with the minimum detection threshold: $Variation = \frac{(\bar{y}_D^{(Threshold)} - \bar{y}_D^{(0.01\ extr)})}{\bar{y}_D^{(0.01\ extr)}} * 100$ (6).

Moreover, microdosimetric dose distributions *d(y)* can be used to assess the Relative Biological Effectiveness for V79 cells irradiated with protons or carbon ions, using a phenomenological weighting function, *r(y)*, by [Parisi et al., 2020] as follows:

$$RBE_{\mu} = \int_{y_{min}}^{\infty} r(y)d(y)\mathrm{d}y \qquad (7)$$

The relative variation on RBE_{μ}, depending on the lowest detection level and application or not of the extrapolation procedure, has been calculated similarly to what is done for $\bar{y}_D$ with equation (6). The biological weighting function used in this work is shown in Figure 2.

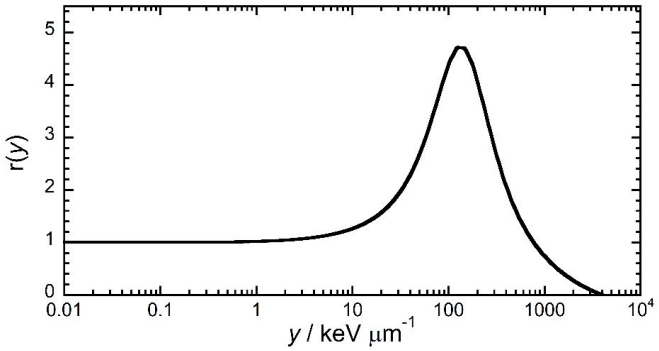

Figure 2 – Biological weighting function from [Parisi et al., 2020].

The meaning of y_{min} in equation (7) is the same as in equations (4) and (5). It should be observed that *r(y)* was determined mainly from simulated spectra, considering y_{min}= 0.016 keV/µm. The latter value corresponds to the simulated lineal energy for one event of one ionization only (10.9 eV) within a spherical water target with diameter equal to 1 µm [Parisi et al., 2020].

3. Results and discussion

In Figure 3 the *yd(y)* spectral distributions of the mini-TEPC in the proton beam (left panel) and carbon ion beam (right panel) are shown after the linear extrapolation down to 0.01 keV/µm.

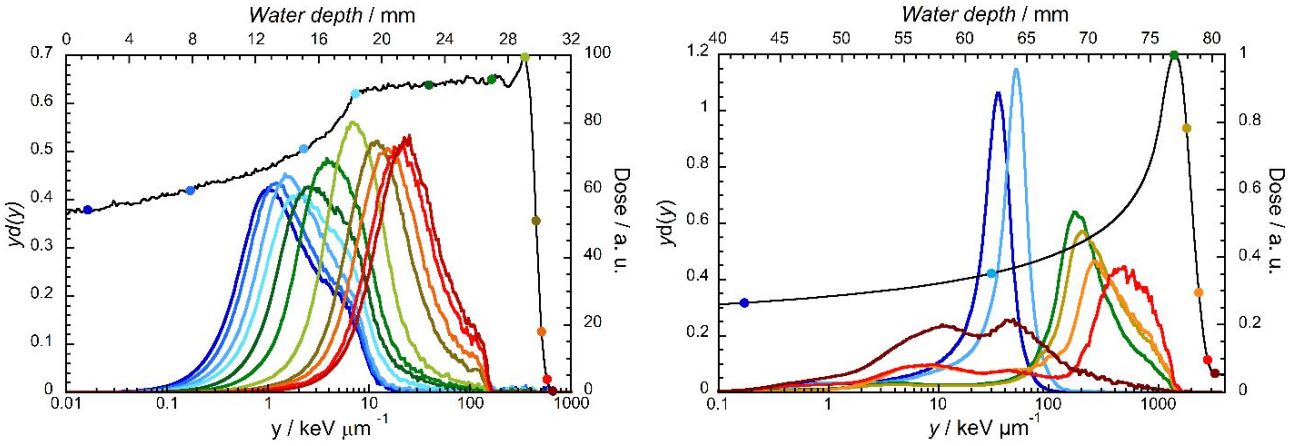

Figure 3 – *yd(y)* distributions in the proton beam (left) and carbon ion beam (right) with the dose profile (black) and the measuring positions marked with the same colours of the spectra.

It is clear from Figure 3 that in the case of the proton beam the most critical spectrum, with respect to the lowest threshold, is the one measured at the smallest depth of 1.4 mm, when the 62 MeV protons deliver a significant fraction of dose through low lineal energy events. In contrast, for carbon ions the most critical spectrum among those shown in Figure 3 is the one measured in the far fall-off region, at depth of 80 mm. Indeed, the fraction of dose imparted by low lineal energy events increases in the fragmentation tail of ^{12}C ion beams, due to the emerging proton component. In the other positions, the contribution from low *y*-events (< 5 keV/µm) to the total dose is below 5%.

Therefore, the effect of different lower detection threshold was studied in detail for protons at depth of 1.4 mm and for carbon ions at depth of 80 mm.

Figure 4 shows *yd(y)* proton distributions (left panel) measured at depth of 1.4 mm and analysed with three different lower level thresholds and consequently three different lineal energy intervals used for linear fitting of experimental data and the relative extrapolation to $y = 0.01$ keV/mm. In the same Figure, the right panel shows the *yd(y)* distributions of the lineal energy measured at depth of 80 mm in the 189.5 MeV/u carbon ions beam and extrapolated to 0.01 keV/µm from 5 different lower level thresholds.

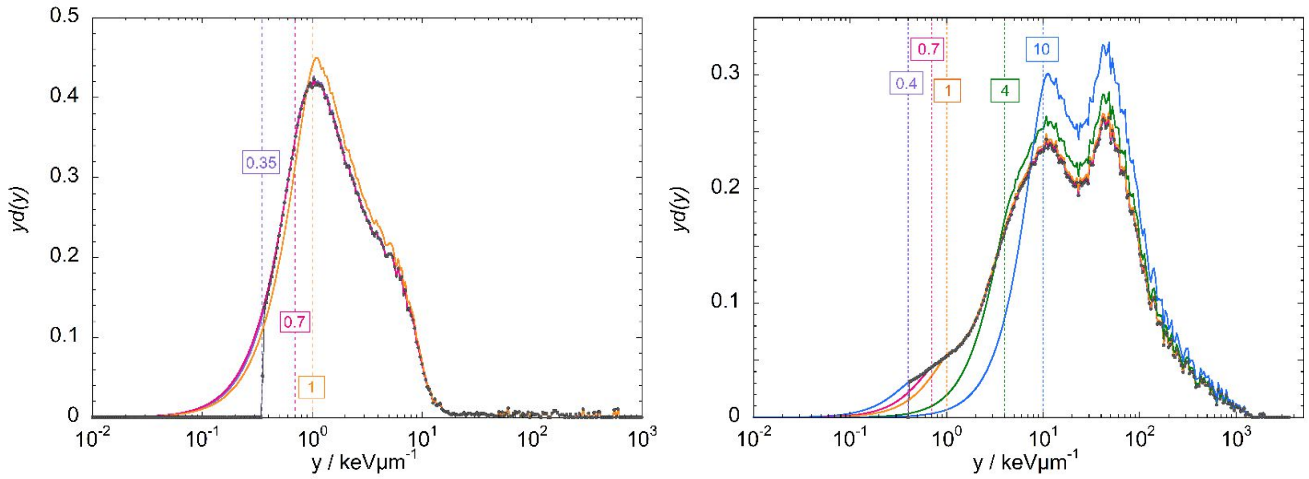

Figure 4 – Left: dose-weighted distributions of the lineal energy measured at depth of 1.4 mm of a 62 MeV modulated proton beam. The experimental minimum detection threshold was 0.35 keV/µm, as determined by electronic noise. Distributions extrapolated from 0.7 and from 1.0 keV/µm are also shown. Right: dose-weighted distributions of the lineal energy measured at depth of 80 mm of a 189.5 MeV/u ^{12}C ion beam. The experimental minimum detection threshold was 0.4 keV/µm, as determined by electronic noise. Distributions extrapolated from 0.4, 0.7, 1.0, 4.0 and 10.0 keV/µm are also shown.

In Figure 5, the same distributions are reported in double-logarithmic scale to better visualize the effect of the different extrapolations.

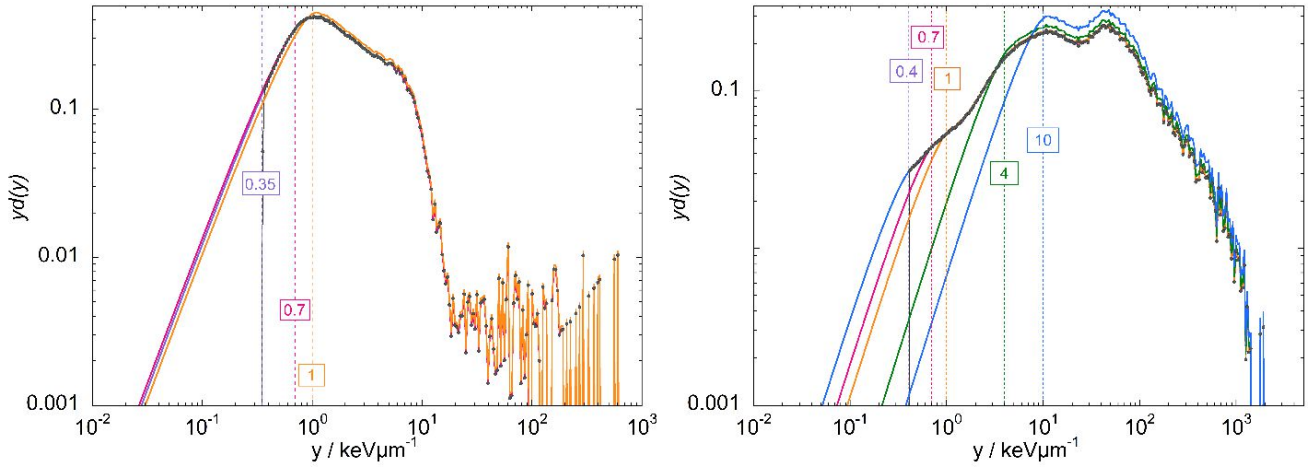

Figure 5 – Same legend as Figure 4, the same figures are reported in double logarithmic scale to better observe the differences in the extrapolated spectra.

As it can be observed in Figures 4 and 5, the effect of considering different lower level thresholds is relevant but the extrapolation procedure can help to recover the missing information due to the detection threshold.

The results obtained for the 11 microdosimetric measurements performed across the 62 MeV modulated proton beam are summarized in Table 2 and Table 3 for the dose-mean lineal energy $\bar{y}_D$, and the RBE_{μ} respectively. Table 4 and 5 show the corresponding results for the 7 microdosimetric measurements performed across the monoenergetic carbon-ion beam.

The second columns of each table report the $\bar{y}_D$ and RBE_{μ} values obtained from equations (4) and (7), with y_{min} = 0.01 keV/μm and considering the distributions obtained by extrapolation of experimental data from 0.35 keV/μm for protons and from 0.4 keV/μm for carbon ions. The other columns report the variation with respect to the data of column 2 obtained without or with extrapolation of the experimental distributions to 0.01 keV/μm at different thresholds.

y_D values for 62 MeV proton beam, obtained with different data processing						
Depth / mm	$\bar{y}_D$ / keV μm^{-1} extrap. 0.35 keV/μm	variation cut 0.35 keV/μm	variation cut 0.7 keV/μm	variation cut 1 keV/μm	variation extrap. 0.7 keV/μm	variation extrap. 1 keV/μm
1.37	3.9 ± 0.2	7.4%	28%	51%	-0.71%	6.0%
7.87	3.9 ± 0.2	5.3%	20%	39%	-1.3%	1.4%

15.06	4.1 ± 0.2	3.4%	13%	24%	-0.11%	-1.3%
18.33	5.3 ± 0.3	2.4%	8.4%	16%	0.25%	-1.1%
23.00	6.4 ± 0.3	1.1%	4.4%	8.7%	0.0%	-0.05%
26.97	7.6 ± 0.4	0.55%	2.1%	4.0%	0.0%	0.15%
29.08	10.9 ± 0.5	0.24%	0.85%	1.5%	0.0%	0.14%
29.78	18.9 ± 0.9	0.10%	0.38%	0.70%	0.0%	0.0%
30.13	23 ± 1	0.07%	0.26%	0.50%	0.0%	0.0%
30.48	30 ± 1	0.05%	0.18%	0.33%	0.0%	0.0%
30.84	33 ± 2	0.02%	0.07%	0.14%	0.0%	0.0%

Table 2 – Relative difference of dose-mean lineal energy calculated from proton microdosimetric distributions with 3 different thresholds and different fitting intervals for extrapolation to 0.01 keV/µm.

In order to facilitate the visualization of the results in Table 2, Figure 6 reports the dose-mean lineal energy values of column 2 in grey dots together with the dose-mean lineal energy value obtained with a threshold of 1 keV/µm (red diamonds) and after the extrapolation from the respective interval (blue triangle). From the plot, it is possible to observe how the extrapolation procedure fully recovers the missing information standing below the threshold.

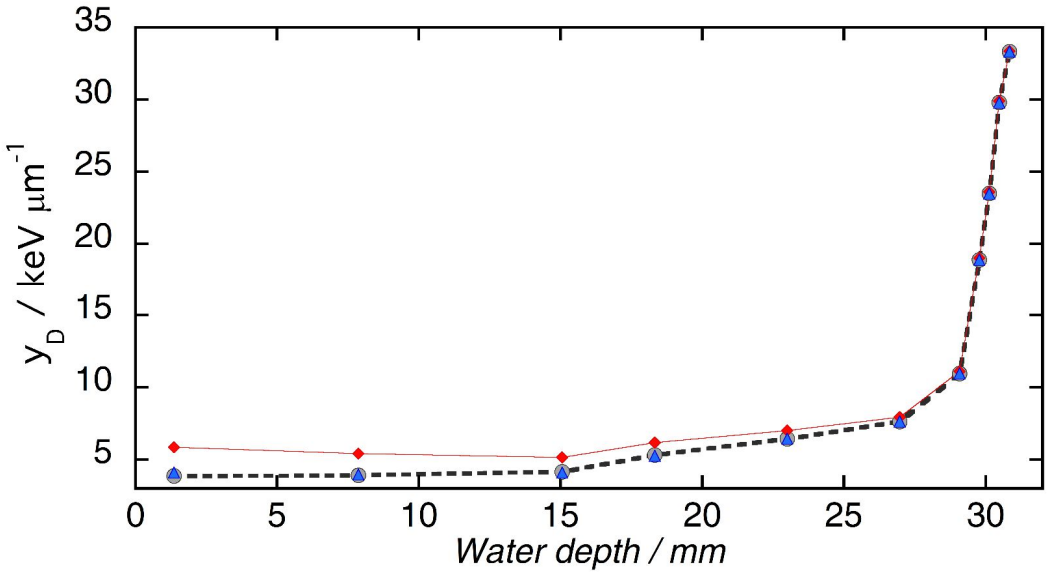

Figure 6 – Dose mean lineal energies extrapolated from 0.35 keV/µm in grey dots, those cut at 1 keV/µm in red diamonds and finally the latter extrapolated down to 0.01 keV/µm in blue triangles as a function of depth in water.

***RBE*µ values for 62 MeV proton beam, obtained with different data processing**						
Depth / mm	*RBE*µ extrap. 0.35 keV/µm	variation cut 0.35 keV/µm	variation cut 0.7 keV/µm	variation cut 1 keV/µm	variation extrap. 0.7 keV/µm	variation extrap. 1 keV/µm

1.37	1.073	0.5%	2.0%	3.6%	-0.1%	0.4%
7.87	1.078	0.4%	1.5%	2.9%	-0.1%	0.1%
15.06	1.089	0.3%	1.1%	2.1%	0.0%	-0.1%
18.33	1.123	0.3%	1.0%	1.8%	0.0%	-0.1%
23.00	1.159	0.2%	0.6%	1.2%	0.0%	0.0%
26.97	1.200	0.1%	0.4%	0.7%	0.0%	0.0%
29.08	1.307	0.1%	0.2%	0.4%	0.0%	0.0%
29.78	1.563	0.0%	0.1%	0.3%	0.0%	0.0%
30.13	1.719	0.0%	0.1%	0.2%	0.0%	0.0%
30.48	1.927	0.0%	0.1%	0.2%	0.0%	0.0%
30.84	2.044	0.0%	0.0%	0.1%	0.0%	0.0%

Table 3 – Relative difference of RBEμ calculated from proton microdosimetric distributions with 3 different thresholds and different fitting intervals for extrapolation to 0.01 keV/μm.

In the same way, the results of Table 3 are reported in Figure 7.

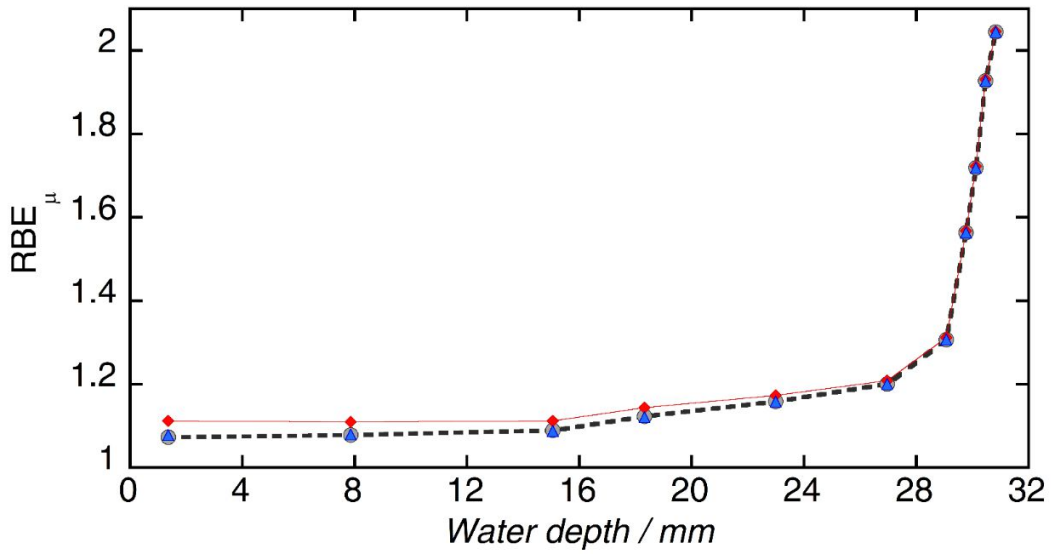

Figure 7 – RBE values extrapolated from 0.35 keV/μm in grey dots, those cut at 1 keV/μm in red diamonds and finally the latter extrapolated down to 0.01 keV/μm in blue triangles as a function of depth in water.

$\bar{y}_D$ values for 189.5 MeV/u carbon ions beam, obtained with different data processing										
Depth / mm	$\bar{y}_D$ / keVμm^{-1} extrap. 0.4 keV/μm	variation cut 0.4 keV/μm	variation cut 0.7 keV/μm	variation cut 1 keV/μm	variation cut 4 keV/μm	variation cut 10 keV/μm	variation extrap. 0.7 keV/μm	variation extrap. 1 keV/μm	variation extrap. 4 keV/μm	variation extrap. 10 keV/μm
42.1	29 ± 1	1.6%	3.4%	4.6%	9.9%	16%	0.73%	1.9%	6.4%	9.7%
62.1	42 ± 2	1.1%	2.3%	3.4%	8.5%	14%	0.22%	0.93%	5.5%	8.3%

76.9	245 ± 12	0.50%	1.0%	1.4%	4.8%	7.7%	0.34%	0.61%	2.2%	5.5%
77.9	303 ± 15	0.42%	0.83%	1.1%	4.0%	6.3%	0.28%	0.51%	1.8%	4.6%
78.9	288 ± 14	0.0%	0.22%	0.42%	5.5%	15%	0.0%	0.0%	0.0%	6.7%
79.6	356 ± 18	1.5%	2.8%	3.8%	11%	22%	0.96%	1.8%	5.0%	12%
80.2	56 ± 3	2.1%	4.1%	5.9%	22%	53%	1.0%	2.1%	8.3%	24%

Table 4 – Maximum variation of dose-mean lineal energy calculated from carbon-ion microdosimetric distributions with 5 different thresholds and different fitting intervals for extrapolation to 0.01 keV/µm.

***RBE*µ values for 189.5 MeV/u carbon ions beam, obtained with different data processing**										
Depth / mm	*RBE*µ extrap. 0.4 keV/µm	variation cut 0.4 keV/µm	variation cut 0.7 keV/µm	variation cut 1 keV/µm	variation cut 4 keV/µm	variation cut 10 keV/µm	variation extrap. 0.7 keV/µm	variation extrap. 1 keV/µm	variation extrap. 4 keV/µm	variation extrap. 10 keV/µm
42.1	1.9	0.8%	1.6%	2.2%	4.8%	7.9%	0.4%	0.9%	3.1%	4.7%
62.1	2.4	0.6%	1.3%	2.0%	4.9%	8.1%	0.1%	0.5%	3.2%	4.9%
76.9	3.2	0.3%	0.7%	0.9%	3.2%	5.1%	0.2%	0.4%	1.5%	3.7%
77.9	2.0	0.3%	0.5%	0.7%	2.5%	4.0%	0.2%	0.3%	1.2%	2.9%
78.9	2.4	0.0%	0.1%	0.2%	3.1%	8.0%	0.0%	0.0%	0.0%	3.7%
79.6	1.9	0.7%	1.3%	1.7%	4.9%	9.1%	0.4%	0.8%	2.2%	5.4%
80.2	2.0	1.0%	2.1%	2.9%	11%	26%	0.5%	1.0%	4.2%	12%

Table 5 – Maximum variation of RBEµ calculated from carbon-ion microdosimetric distributions with 5 different thresholds and different fitting intervals for extrapolation to 0.01 keV/µm.

It is possible to observe from Table 2 that the value of $\bar{y}_D$ calculated from the proton experimental *d(y)* distributions with a lower cut at 1 keV/µm (without extrapolation) is 50% higher than the value calculated with *d(y)* distributions extrapolated from 0.35 keV/µm to 0.01 keV/µm. The difference is reduced to 5% if extrapolation from 1 keV/µm to 0.01 keV/µm is also performed.

For carbon ions data, whose results are shown in Table 4, differences in $\bar{y}_D$ are always smaller than 6%, for distributions cut at y_{min} = 1 keV/µm, and even smaller when the extrapolation to 0.01 keV/µm is performed. Summarizing, up to a threshold of 1 keV/µm, all results, both from the cut and extrapolated distributions, differ by less than 5%. When higher thresholds are used, differences in the fragmentation tail of the ^{12}C ions beam rise up to 54%. The differences increase with increasing threshold values, but are always strongly reduced if the extrapolation procedure is applied. It is therefore advisable to carry out the extrapolation procedure, in order to compare the results collected with different set-ups characterized by different noise conditions and lower detection thresholds.

From Tables 3 and 5 it is noticeable that the lower threshold has a reduced influence on the RBE_{μ} calculated values. In particular, considering a lower detection threshold of 1 keV/µm and distributions extrapolated from 1 keV/µm to 0.01 keV/µm, the differences in RBE_{μ} are always smaller than 0.5% for protons and 1% for carbon ions.

4. Conclusions

Measurements are always affected by electronic noise that determines the minimum detectable signal. In microdosimetry with solid state detectors, for instance, a lower detection threshold at y = 1 keV/µm is frequently reported, while with tissue equivalent proportional counters the lower threshold can be smaller, thanks to the amplification of the gas avalanche. When comparing the mean values of the lineal energy distributions, care should be taken for the lower detection threshold, because neglecting a significant portion of the distribution (the part below the noise level) results in an overestimation of the mean values. In this work, it has been shown that a lower detection threshold at 1 keV/µm results in an overestimation of 50% for $\bar{y}_D$ for 62 MeV protons at small depths. The situation is less severe for carbon ion beams, apart from measurements performed in the region beyond the Bragg peak where the dose is delivered mainly by secondary protons. Differences in the entrance part of the SOBP due to different analysis procedure could lead to an overestimation of the dose delivered to skin and healthy tissues between the entrance of the beam and the tumour that could imply an underestimation of the dose to the tumour to avoid complications in the shallow depths. Similar consideration applies to the fall off region, beyond the Bragg peak.

Furthermore, the extrapolation of the experimental distributions to a common value of 0.01 keV/µm was proven to significantly reduce the deviations in the mean values due to the different lower thresholds. It is therefore recommended to extrapolate experimental distributions down to the minimum value of 0.01 keV/µm, before calculating the dose-mean lineal energy values.

Differences in the determination of RBE using the biological weighting function for extrapolated or non-extrapolated spectra are always less than 5%, apart from the cut at 4 keV/µm and 10 keV/µm in the distal region of the carbon ions dose profile. Therefore, these differences might be not clinically observable in most cases (apart from the falloff region, which is of relevance to evaluate side effects due to irradiation of healthy tissue behind the tumour). However, differences could possibly be bigger, for example, if the modified microdosimetric kinetic model (MKM) is used instead of the biological weighting function

approach, so that large differences in the mean values of the dose distribution can easily lead to wrong RBE estimations.

All the values found in this paper refer to these two radiation fields and a mini-TEPC. The variations due to threshold and extrapolation may vary in different radiation fields or when measuring with different detectors and for this reason it is advisable to perform an evaluation case by case. Moreover, at least one measurement with higher sensitivity should be performed (higher gas gain for TEPC, or thicker active layer for solid state microdosimetry), in order to verify that no relevant structure is present in the part of the microdosimetric distribution that remains below the threshold, where the detection system is not sensitive. This last procedure is highly recommended in mixed radiation fields where more than one component can be found in the spectrum.

Acknowledgement

This work was supported by the 5th Scientific Commission of the Italian Institute for Nuclear Physics (INFN), the Belgian Nuclear Research Centre SCK CEN and Hasselt University. This work has been partially supported by the ENEN+ project that has received funding from the EURATOM research and training Work Programme 2016 – 2017 – 1 #755576.

References

- Agosteo, S., et al., *Study of a silicon telescope for solid state microdosimetry: preliminary measurements at the therapeutic proton beam line of CATANA.* Radiat. Meas. 45, 1284–1289 (2010).

- Beck P et al., *Cosmic radiation exposure of aircraft crew: Compilation of measured and calculated data*, Appendix A. Radiation Protection Issue No. 140. European Commission (2004).
- Bianchi A. et al., *Microdosimetry with a sealed mini-TEPC and a silicon telescope at a clinical*
- *proton SOBP of CATANA*, Radiation Physics and Chemistry 171, 108730 (2020).
- Bianchi A. et al., *Lineal energy calibration of a mini-TEPC via the proton-edge technique*, Radiat. Meas. 141 106526 (2021).

- Booz J. et al., ICRU Report 36: Microdosimetry, *Journal of the International Commission on Radiation Units and Measurements*, Volume 19, Issue 1, Bethesda (1983)

- Cirrone G.A. P. et al., *A 62-MeV proton beam for the treatment of ocular melanoma at Laboratori Nazionali del Sud-INFN*. IEEE Trans. Nucl. Sci. 51 (3), 860–865 (2004).

- Conte V. et al., *Mini-TEPC Microdosimetric Study of Carbon Ion Therapeutic Beams at CNAO* EPJ Web Conf. Volume 153, (2017). DOI:10.1051/EPJCONF/201715301012
- Conte V. et al., *Microdosimetry at the CATANA 62 MeV proton beam with a sealed miniaturized TEPC*. Phys. Med. 62, 114–122 (2019).
- Conte V. et al., *Microdosimetry of a therapeutic proton beam with a mini-TEPC and a MicroPlus-Bridge detector for RBE assessment,* Phys. Med. Biol. 65, 245018 (2020).

- Debrot, E. et al.. *SOI microdosimetry and modified MKM for evaluation of relative biological effectiveness for a passive proton therapy radiation field.* Phys. Med. Biol. 63 (2018).
- De Nardo L. et al., *Mini-TEPCs for radiation therapy*. Radiat. Protect. Dosim. 108 (4), 345–352 (2004).

- Durante M. *Biological Effects of Densely Ionizing Radiation*. In: Dössel O., Schlegel W.C. (eds) World Congress on Medical Physics and Biomedical Engineering, September 7 - 12, 2009, Munich, Germany. IFMBE Proceedings, vol 25/3. Springer, Berlin, Heidelberg. https://doi.org/10.1007/978-3-642-03902-7_72 (2009)

- Lindborg, L., *Microdosimetry measurements in beams of high energy photons and electrons: technique and results*, SSI--1975-025 (1975).
- Lindborg L. and Waker A., *Microdosimetry: Experimental Methods and Applications*, Apple Academic Press Inc. (2017)
- Missiaggia M. et al., *Microdosimetric measurements as a tool to assess potential in-field and out-of-field toxicity regions in proton therapy*. Phys Med Biol. 65(24):245024. doi: 10.1088/1361-6560/ab9e56. PMID: 32554886 (2020).
- Moro et al., *Statistical and overall uncertainties in BNCT microdosimetric measurements,* LNL-INFN(REP)-199/2003 (2003a)
- Moro et al., *Statistical and overall uncertainties in proton therapy microdosimetric measurements,* LNL-INFN(REP)-200/2003 (2003b)

- Parisi et al., *Development of a new microdosimetric biological weighting function for the RBE10 assessment in case of the V79 cell line exposed to ions from* ^{1}H *to* ^{238}U, Phys. Med. Biol. 65 235010 (2020).

- Rossi, H.H., *Microdosimetry. Biophysical aspects of radiation quality* - International Atomic Energy Agency (IAEA): IAEA. - inis.iaea.org (1966).

- Rossi H.H. and Zaider M., *Microdosimetry and its application,* Springer (1996).

- D. Srdoc, *Experimental Technique of Measurement of Microscopic Energy Distribution in Irradiated Matter Using Rossi Counters,* Radiat. Res., 43(2), 302-319, (1970).

- Verona C. et al., *Microdosimetric measurements of a monoenergetic and modulated Bragg Peaks of 62 MeV therapeutic proton beam with a synthetic single crystal diamond microdosimeter*. Med. Phys., 47: 5791-5801. https://doi.org/10.1002/mp.14466 (2020)